

Research on Polycrystalline Thin-Film CuGaInSe₂ Solar Cells

Annual Subcontract Report 3 May 1991 – 2 May 1992

NREL/TP--413-5012

DE92 016439

B.J. Stanbery, W.S. Chen, W.E. Devaney,
J.M. Stewart
*Boeing Defense & Space Group
Seattle, Washington*

NREL technical monitor: H.S. Ullal



National Renewable Energy Laboratory
1617 Cole Boulevard
Golden, Colorado 80401-3393
A Division of Midwest Research Institute
Operated for the U.S. Department of Energy
under Contract No. DE-AC02-83CH10093

MASTER

Prepared under Subcontract No. ZH-1-19019-6

November 1992

EP

This publication was reproduced from the best available camera-ready copy submitted by the subcontractor and received no editorial review at NREL.

On September 16, 1991 the Solar Energy Institute was designated a national laboratory, and its name was changed to the National Renewable Energy Laboratory.

NOTICE

This report was prepared as an account of work sponsored by an agency of the United States government. Neither the United States government nor any agency thereof, nor any of their employees, makes any warranty, express or implied, or assumes any legal liability or responsibility for the accuracy, completeness, or usefulness of any information, apparatus, product, or process disclosed, or represents that its use would not infringe privately owned rights. Reference herein to any specific commercial product, process, or service by trade name, trademark, manufacturer, or otherwise does not necessarily constitute or imply its endorsement, recommendation, or favoring by the United States government or any agency thereof. The views and opinions of authors expressed herein do not necessarily state or reflect those of the United States government or any agency thereof.

Printed in the United States of America
Available from:
National Technical Information Service
U.S. Department of Commerce
5285 Port Royal Road
Springfield, VA 22161

Price: Microfiche A01
Printed Copy A03

Codes are used for pricing all publications. The code is determined by the number of pages in the publication. Information pertaining to the pricing codes can be found in the current issue of the following publications which are generally available in most libraries: *Energy Research Abstracts (ERA)*; *Government Reports Announcements and Index (GRA and I)*; *Scientific and Technical Abstract Reports (STAR)*; and publication NTIS-PR-360 available from NTIS at the above address.

DISCLAIMER

**Portions of this document may be illegible
electronic image products. Images are
produced from the best available original
document.**

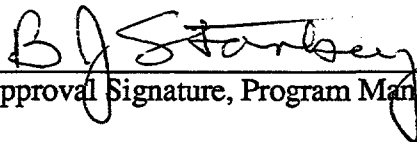
PREFACE

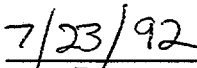
For the past several years, The Boeing Company has conducted pioneering research and development of CuInSe_2 and CuInGaSe_2 polycrystalline thin film solar cells. We have consistently demonstrated state-of-the-art efficiency for these thin film solar cells. The results reported herein for our work during the first phase of this contract demonstrate that we are continuing this tradition of technology leadership today.

In addition, Boeing has effectively transferred the technology for high efficiency cell preparation to other research organizations. With the very small worldwide resource base available for CuInSe_2 cell development, this technology transfer contribution is extremely significant to the future, successful advancement of these attractive polycrystalline thin-film solar cells.

Most recently, Boeing has conducted an in-depth study of the prospects for and obstacles to the scale-up of our currently implemented technology to manufacturing, under the auspices of the Photovoltaic Manufacturing Technology Initiative, in the course of our Phase 1 contract. This analysis demonstrated that the methods we are developing in the context of this and prior cost-shared NREL contracts, as well as complimentary research funded exclusively by Boeing, have the potential to achieve the DOE's cost goals for photovoltaic electrical power generation by the end of this decade.

The authors would like to acknowledge the critical contributions of Richard Murray, Rex Armstrong and Dan Peterson to this work. Each and together they have provided the infrastructure for and much of the execution of the work reported herein. We would also like to acknowledge Reid Mickelsen and Robert Burgess for their constructive review of the manuscript for this report.


Approval Signature, Program Manager


Date

SUMMARY

OBJECTIVES

The objectives of this research effort are to fabricate high efficiency CdZnS/CuGaInSe₂ thin film solar cells, and to develop improved transparent conductor window layers such as ZnO. Our specific technical milestone for Phase I was the demonstration of an AM1.5 global 13%, 1cm² total area CuGaInSe₂ thin film solar cell. In addition, we have delivered optimized CuGaInSe₂ solar cells and CuGaInSe₂ films on Mo-metallized substrates biannually.

DISCUSSION

Analysis of the properties of the best ZnO/CdZnS/CuInGaSe₂ cells developed by Boeing for SERI under a prior subcontract suggested that significant performance improvements could be realized by further optimization of the thin CdZnS layer to reduce shunt currents while maintaining subbandgap transparency, the ZnO layer to reduce IR absorption while maintaining adequate lateral conductivity, and the CuInGaSe₂ (CIGS) layer to optimize gallium content and gradients along with minority carrier transport properties.

During the early portion of this contract phase our activities were focused on three areas. First, our CIGS deposition system was modified to double its substrate capacity. This increased throughput has proven critical to speeding the pace of process development by providing multiple substrates from the same CIGS run which can be used to reduce uncertainty in the cause of differences resulting from the intentional variation of other process parameters. Second, new tooling was developed to enable investigation of a modified aqueous CdZnS process whose goal was to improve the yield of this critical step in the device fabrication process. Third, our ZnO sputtering system was upgraded to improve its reliability, and the sputtering parameters further optimized to improve its properties as a Transparent Conducting Oxide (TCO).

Characterization of the new CIGS deposition system substrate fixturing was completed. After some troubleshooting and modification, good thermal uniformity and adequately high temperatures for device-quality CIGS deposition were achieved. Optimization of the modified aqueous Cd_{1-y}Zn_yS process has enabled us to reproducibly deposit adherent, substantially pinhole-free films over a 2"x2" substrate for zinc fractions in the range $0 \leq y \leq 0.30$. The electro-optical properties of the ZnO were improved, enabling the use of thinner layers while preserving high light generated currents and fill factors.

CONCLUSIONS

Our best *prior* cell fabricated at Boeing was a ZnO/Cd_{0.83}Zn_{0.18}S/CuIn_{0.72}Ga_{0.28}Se₂ cell with an AM1.5 efficiency of 12.5%. Combining the refined CdZnS process with CIGS from the newly fixtured deposition system enabled us to fabricate and deliver an 11.5% efficient, 4 cm², ZnO/Cd_{0.81}Zn_{0.18}S/CuIn_{0.71}Ga_{0.29}Se₂ cell. Further refinement of both the CIGS and ZnO deposition processes has enabled us fabricate a ZnO/Cd_{0.82}Zn_{0.18}S/CuIn_{0.80}Ga_{0.20}Se₂ cell whose I-V characteristics and derived parameters as measured at NREL under standard test conditions gave 13.1% efficiency with V_{oc} = 0.518 volts, I_{sc} = 34.1 mA, FF = 0.728 and a cell area of 0.979 cm². This NREL measurement verifies that we have met our key technical milestone for Phase 1. Furthermore, we have delivered to NREL 6 each ~1 cm² CuIn_{1-x}Ga_xSe₂ cells which are 12-13% in efficiency with gallium contents in the range $0.20 \leq x \leq 0.26$.

TABLE OF CONTENTS

	<u>Page</u>
1.0 Introduction.....	1
2.0 Methods	3
2.1 Cu(In,Ga)Se ₂	3
2.2 CdZnS Chemical Deposition.....	3
2.3 ZnO Layer Deposition	3
2.4 MgF ₂ Antireflection Coating	4
3.0 Technical Discussions	6
3.1 Process Options and Device Performance.....	6
3.1.1 Substrate Temperature.....	6
3.1.2 Zinc content in CdZnS.....	8
3.1.3 ZnO Layer.....	9
3.2 Device Analysis.....	10
3.2.1 Light Generated Current.....	10
3.2.2 Open Circuit Voltage.....	12
3.2.3 Fill Factor	13
4.0 Conclusions.....	14
5.0 References.....	15

LIST OF FIGURES

Figure 1-1.	Structure of ZnO/CdZnS/CuInGaSe ₂ solar cells	1
Figure 1-2.	I-V characteristics of cell 1490AD as measured at NREL.....	2
Figure 2-1.	Diffuse + Specular Reflection from ZnO/CdZnS/CuInGaSe ₂ cell #1490AC.....	4
Figure 2-2.	Quantum Efficiency for ZnO/CdZnS/CuInGaSe ₂ cell 1490AC before (solid) and after (dashed) MgF ₂ antireflection coating. Coating is quarter wave at approximately 700 nm.....	5
Figure 3-1.	SEM photograph of CuIn _{1-x} Ga _x Se ₂ grown with a final substrate temperature of 500°C. Cu/(In+Ga) = 0.891, with x = 26.8%.....	6
Figure 3-2.	SEM photograph of CuIn _{1-x} Ga _x Se ₂ grown with a final substrate temperature of 530°C. Cu/(In+Ga) = 0.894, with x = 26.6%.....	7
Figure 3-3.	Optical absorption of the ZnO layer as used in the high efficiency cells. Derived from measurement of diffuse + specular reflectance and transmission on a P-E Lambda-9.....	9
Figure 3-4.	Quantum Efficiency of Cell 1490AD with 20% gallium (solid line) compared with cell 1174H with 28% gallium (dashed line).	10
Figure 3-5.	Cell 1490AC reflectance and quantum efficiency. The various curves are identified in the text.....	11

LIST OF TABLES

Table 3-1.	Performance of ZnO/Cd _{1-y} Zn _y S/CuIn _{1-x} Ga _x Se ₂ cells with varied gallium (x) and zinc (y) molar fractions	8
Table 3-2.	The effect on efficiency of removing the major quantified loss mechanisms in the present cells, as measured on cell #1490AC.....	12
Table 3-3.	Current-Voltage characteristics of the 4 cells made on the substrate which yielded the highest efficiency	13

1.0 INTRODUCTION

This is the First Annual Technical Progress Report on our activities and achievements in Phase 1 of a three-year, phased research program entitled "Research on Polycrystalline Thin Film CuGaInSe₂ Solar Cells." The work reported herein was conducted in the period between May 3, 1991 and May 2, 1992. This work continues the research performed under several previous contracts and focuses on further development of thin film polycrystalline heteroface solar cells using the mixed alloy Copper Indium Gallium diSelenide (CIGS or CuIn_{1-x}Ga_xSe₂) as the *p*-type absorber layer and Cadmium Zinc Sulfide (Cd_{1-y}Zn_yS) mixed alloys as the *n*-type contact layer with an overlayer of ZnO transparent conducting oxide (TCO) for majority carrier collection to the grids. This ZnO/CdZnS/CuInGaSe₂ semiconductor structure is deposited sequentially onto molybdenum-coated alumina substrates by different processes, and finished with a top grid structure composed of gridlines and buss bars. Aluminum is used for the grid material and nickel is used as the contact layer between the aluminum and the ZnO. This cell structure is shown schematically in figure 1-1.

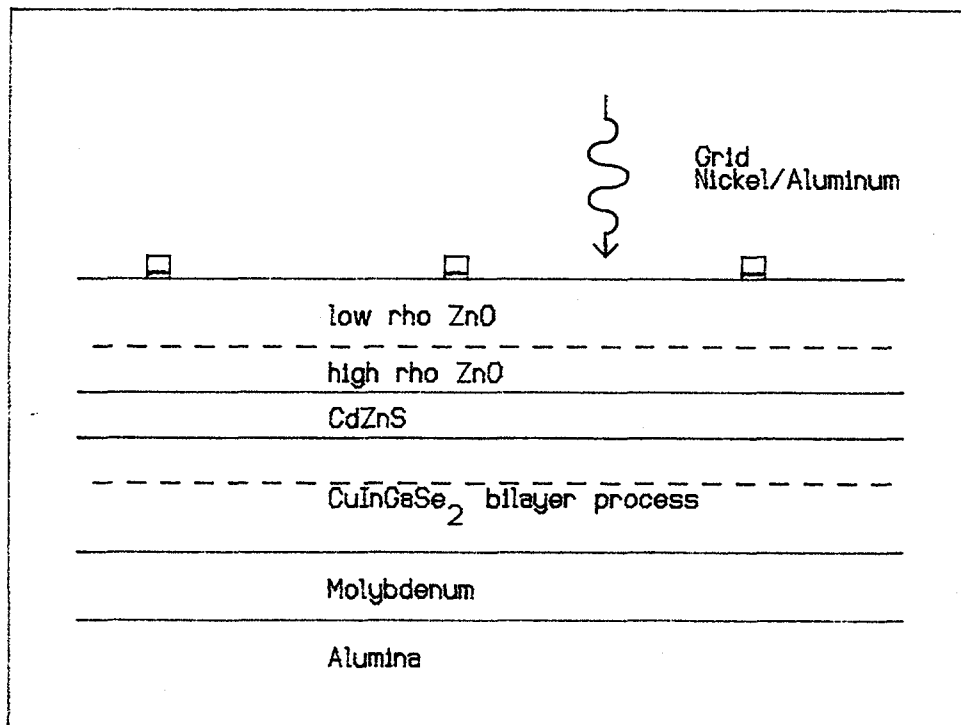


Figure 1-1. Structure of ZnO/CdZnS/CuInGaSe₂ solar cells

An Anti-Reflection Coating (ARC) of MgF₂ has also been deposited onto some of the best cells we have fabricated during this phase in order to reduce reflection losses and improve their performance.

Our best prior cell fabricated at Boeing was a ZnO/Cd_{0.83}Zn_{0.17}S/CuIn_{0.72}Ga_{0.28}Se₂ cell with an AM1.5 efficiency of 12.5%. During this phase of our contract we have fabricated and delivered to NREL cells over 13% in efficiency with gallium contents in the range $0.20 \leq X \leq 0.26$ (figure 1-2.)

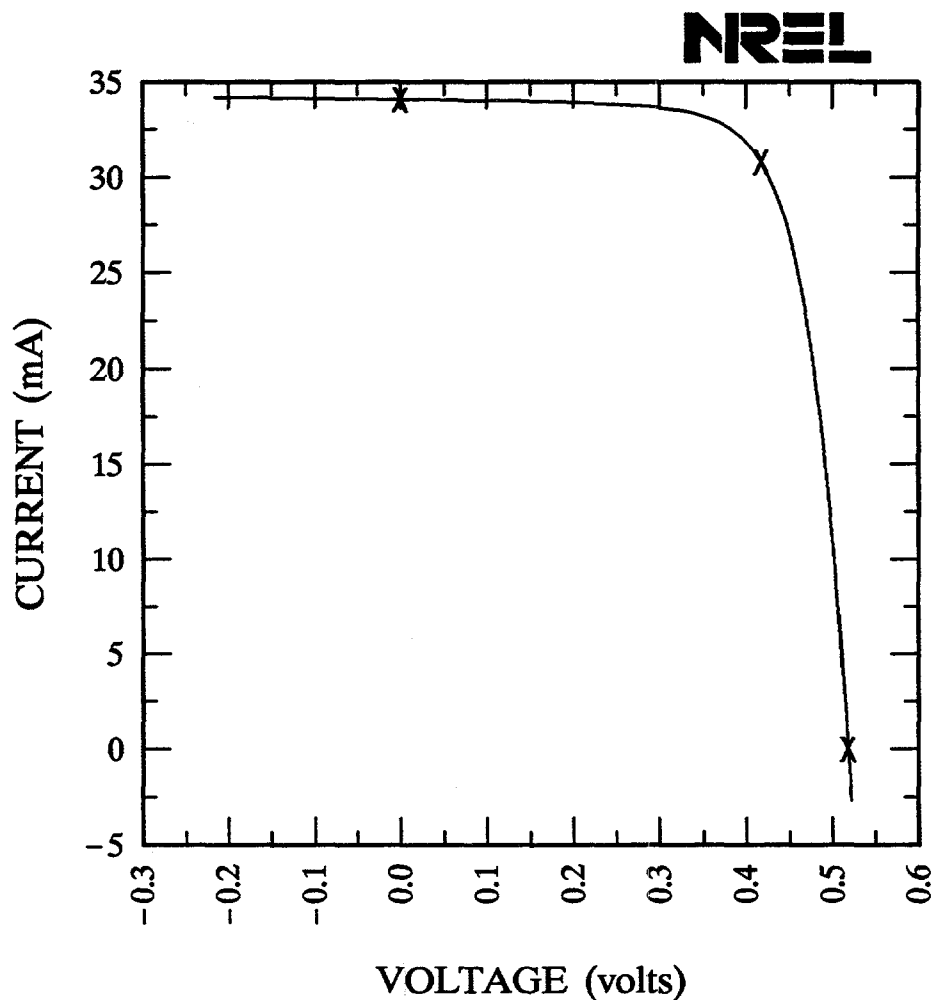
Boeing, ZnO/CdZnS/CuInGaSe₂/Mo, global

Sample: 1490A-D

Temperature = 25.0°C

Mar. 12, 1992 9:38 am

Area = 0.979 cm²



$V_{oc} = 0.5184$ volts

$I_{sc} = 34.07$ mA

$J_{sc} = 34.80$ mA/cm²

$P_{max} = 12.86$ mW

Fill factor = 72.82 %

$I_{max} = 30.79$ mA

Efficiency = 13.1 %

$V_{max} = 0.4177$ V

Figure 1-2. I-V characteristics of cell 1490AD as measured at NREL.

2.0 METHODS

2.1 CU(IN,GA)SE₂

Our CuInGaSe₂ films are prepared by multisource simultaneous elemental deposition onto heated molybdenum-coated alumina substrates. This procedure is described in detail in reference [1]. The material evaporation rates are controlled by a combination of EIES and quartz crystal sensors which determine film composition. In order to ameliorate the composition gradient effects resulting from the spatial separation of the sources, the substrates are rotated. The substrate rotation also assists in removing temperature gradients due to the nonuniformity of the heater lamp illumination. The selenium is evaporated to excess to produce suitable material. The substrate temperature ranges from 450–500°C for the first deposited layer and 500–550°C for the second layer. The system pressure is approximately 10⁻⁶ millibar.

The substrate temperature has a significant effect on the film composition. For a constant material flux on the substrate, an increase in the substrate temperature will result in a loss of indium in the film with a resultant change in film composition. Careful control of the substrate temperature is important for run to run reproducibility. During the past contract year significant effort was devoted to redesign of the substrate heater. We availed ourselves of this opportunity to modify the substrate holder to accommodate four 2" by 2" substrates instead of two. Four nearly identical selenide coated substrates can now be produced. This greater throughput of the system facilitates the evaluation of the ZnO and CdZnS layers. Due to the above changes and improvements in the operating procedures, four recent consecutive runs resulted in devices with efficiencies from 11% to over 13% for AM1.5G conditions.

2.2 CDZNS CHEMICAL DEPOSITION

The chemical deposition of thin CdZnS film is essentially unchanged from previous work [2]. Refinements have been made during this contract. A new stainless steel sample holder has been made and used, which can accommodate maximum number of four 2x2 inch samples or eight 1x2 samples. Premixed solution of CdCl₂, ZnCl₂ and thiourea are brought to the temperature of 80–90°C under stirring. Substrates are then immersed into the solution after a proper amount of NH₄OH is added. The reaction in the solution goes to completion in approximately 30–40 minutes during which time deposition of a film of 20–30 nm occurs.

Immediately after the samples are removed from the solution they are ultrasonically cleaned, rinsed in deionized water and blown dry with nitrogen. Samples are subjected to 5 minutes bake in oxygen at 200°C immediately before the subsequent ZnO deposition process step.

2.3 ZNO LAYER DEPOSITION

The ZnO films are deposited in an inline system by RF magnetron sputtering onto the moving substrate in an argon or mixed oxygen and argon atmosphere. The details of the deposition process were described in reference [2]. In this work, the high resistivity (≤ 10 Ω-cm) layer is approximately 50 nm thick. The low resistivity layer (approximately 300 nm in thickness) has a sheet resistivity of 25–65 Ω/square depending on the oxygen content in the sputtering atmosphere. The lower resistivity (25 Ω/square) layer is less transparent than the higher resistivity

(65 Ω /square) layer. The optical transmission characteristics of the ZnO layers and their effects on cell performance will be discussed in section 3.1.3 .

2.4 MgF_2 ANTIREFLECTION COATING

Antireflection coating of the present cells is substantially different from that for the conventional CdZnS/CuInSe₂ cells. The ZnO/CdZnS/CuInGaSe₂ cell structure by itself is relatively effective in suppressing the reflection which would be expected from a bare selenide surface. The index of the ZnO is close to the geometric mean of the selenide and air. The thin sulfide layer is thin enough to have relatively little effect on the optical interaction between ZnO and the selenide. In spite of these considerations the net reflection loss in the cell is still approximately 5% and large enough to warrant further reduction.

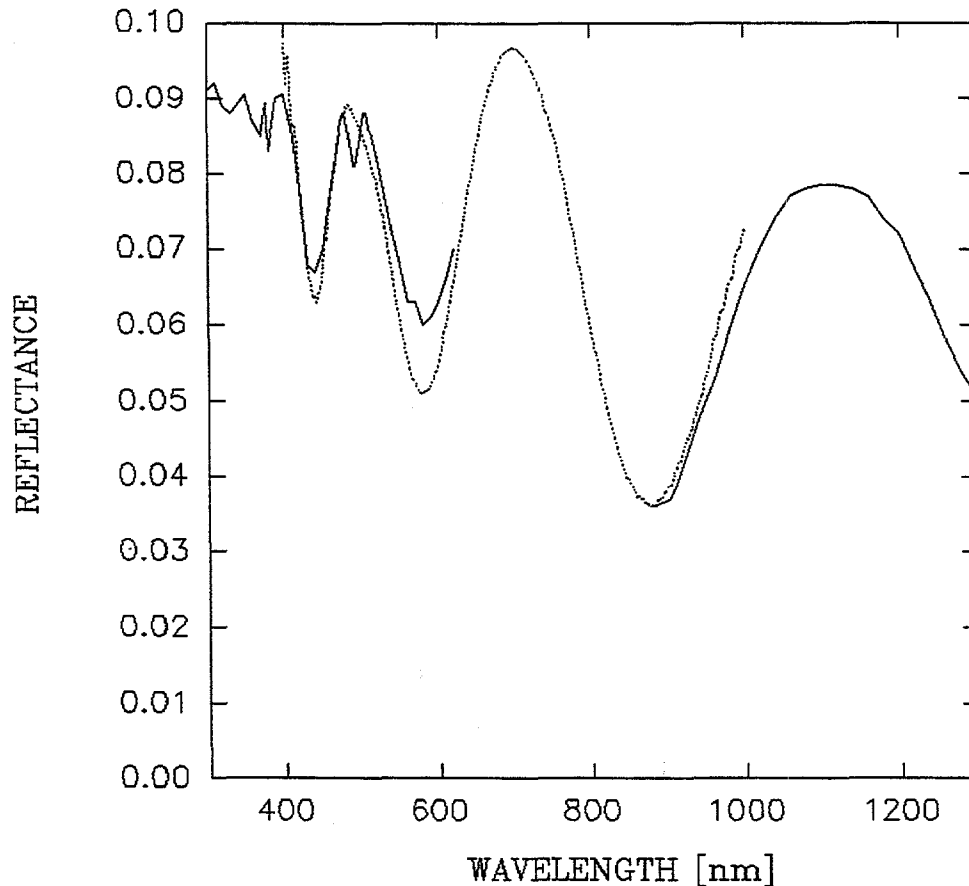


Figure 2-1. Diffuse + Specular Reflection from ZnO/CdZnS/CuInGaSe₂ cell #1490AC

In figure 2-1 the three sections correspond to measurements on Perkin-Elmer Lambda-9, Li-Cor LI-1800 and P-E Lambda-9 instruments, respectively. The measurements include grid reflectance. The ZnO layer is optically coherent and at 700 nm is approximately 3 quarter-wavelengths optical thickness. The optical interference which results is clearly seen in the reflection from this cell.

Magnesium fluoride, MgF_2 , is well suited as a single layer antireflection coating on ZnO. The low resistivity ZnO has an index of refraction of approximately 1.9 in the wavelength range near 700 nm. MgF_2 has an index of 1.38 when deposited by physical vapor deposition and therefore

will give essentially zero reflection at a single wavelength when deposited on bulk ZnO. Such a structure is the classic case of a quarter wave single layer antireflection coating with the index of refraction of the antireflection layer equal to the square root of the substrate [3]. The problem with the ZnO/CdZnS/CuInSe₂ or ZnO/CdZnS/CuInGaSe₂ system is that the ZnO does not even approximate the bulk substrate condition described above. We are therefore depositing the MgF₂ onto the thin, optically coherent ZnO layer, not onto a semi-infinite ZnO surface. The resulting optical interaction between the quarter wavelength MgF₂ layer and the three quarter wavelength ZnO layer results in a decrease in reflection at 700 nm but actually gives an increase in reflection at some other wavelengths. The net result of such a MgF₂ layer is shown in figure 2-2 for one test cell. The quantum efficiency before and after AR deposition is shown. The MgF₂ layer used is thicker than that normally used but the effect of the coating is clear. Both the increase in collection at the target wavelength (700 nm) and the decrease at some other wavelengths is clearly seen.

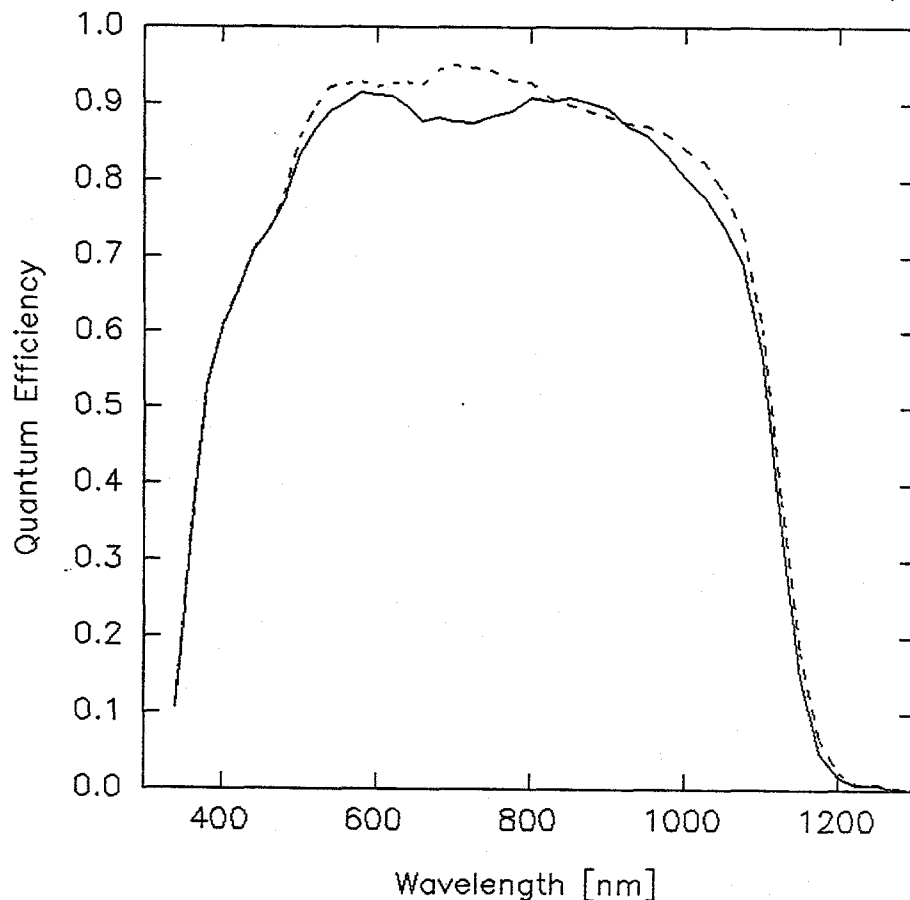


Figure 2-2. Quantum Efficiency for ZnO/CdZnS/CuInGaSe₂ cell 1490AC before (solid) and after (dashed) MgF₂ antireflection coating. Coating is quarter wave at approximately 700 nm.

In spite of the complicated optical effects there is some net gain in collection. We have found that an optimized MgF₂ layer gives a net increase in light generated current of approximately 2.5%. Uncoated glass would also reduce reflection losses from the ZnO surface with the appropriate choice of an index matching adhesive layer, but at the cost of an overall 4% reflection loss at the front surface of the glass.

3.0 TECHNICAL DISCUSSIONS

3.1 PROCESS OPTIONS AND DEVICE PERFORMANCE

3.1.1 Substrate Temperature

As mentioned in section 2.1 the substrate temperature has a dramatic effect on the film properties for a constant incident material flux. An increase in substrate temperature with other variables *constant* will result in a decrease in indium content in the film. This film with lower indium will be composed of somewhat larger grain size and lower resistivity than a film deposited with a lower substrate temperature.

The following figures show the effect on grain size due to a 30°C variation in substrate temperature, but with the incident elemental fluxes adjusted to offset the effect of lower indium incorporation efficiency. The grains for the lower final substrate temperature are of the order of one micron or less. The grain size for the higher temperature substrates are on the order of 5 microns. Note that the Group I / III ratio and gallium molar fraction are nearly identical.

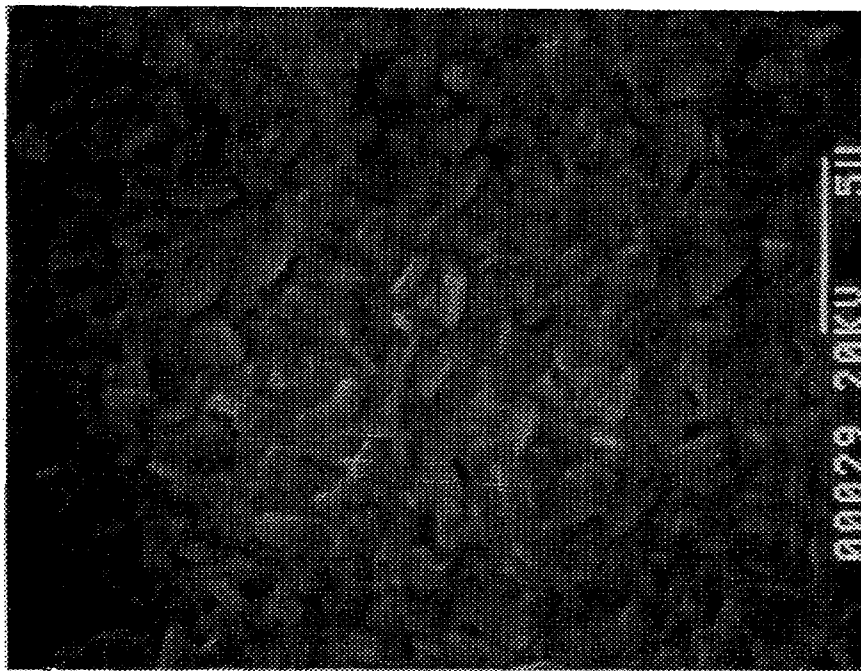


Figure 3-1. SEM photograph of $\text{CuIn}_{1-x}\text{Ga}_x\text{Se}_2$ grown with a final substrate temperature of 500°C. $\text{Cu}/(\text{In}+\text{Ga}) = 0.891$, with $x = 26.8\%$.

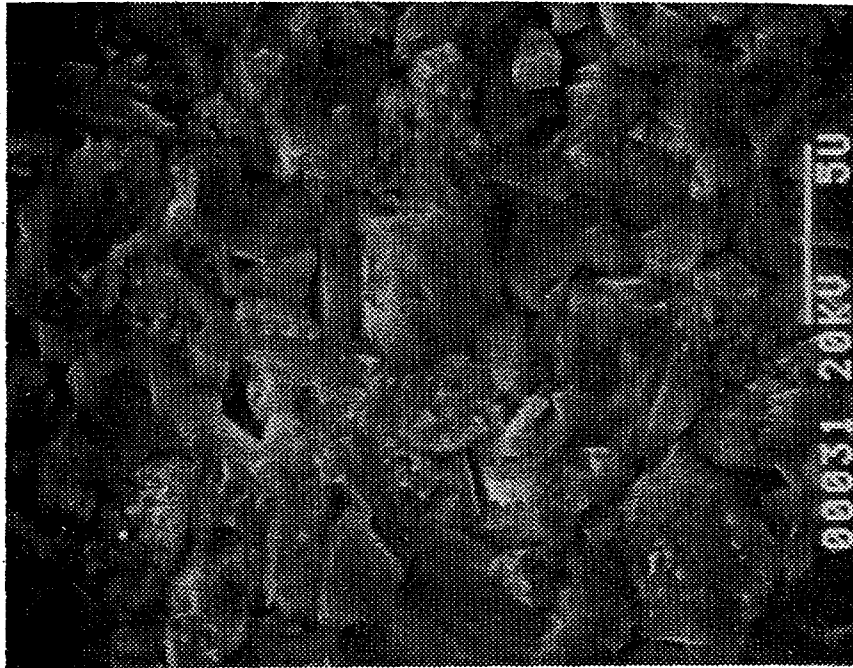


Figure 3-2. SEM photograph of $\text{CuIn}_{1-x}\text{Ga}_x\text{Se}_2$ grown with a final substrate temperature of 530°C . $\text{Cu}/(\text{In}+\text{Ga}) = 0.894$, with $x = 26.6\%$.

During the early period of this contract, runs were made with final substrate temperatures up to 500°C . These runs yielded devices in the range of 8 to 11% efficiency under AM1.5 conditions. In the later portion of this contract phase, the substrate temperature was increased ~ 30 degrees centigrade. Efficiencies for some of these devices exceeded 13% under AM1.5 conditions, and were characterized by higher fill factors and open circuit voltages. Apparently, relatively small absolute deposition temperature changes can significantly change the morphology and improve the electronic properties of these films.

3.1.2 Zinc content in CdZnS

The zinc content (y) in the $Cd_{1-y}Zn_yS$ films deposited by aqueous Chemical Bath Deposition (CBD) have been measured to be nearly identical to the ratio of the molar concentrations $[Zn]/\{[Cd]+[Zn]\}$ in the solution by Auger microprobe analysis [2.1]. Hence, the zinc content can be directly varied by adjusting the ratio of $ZnCl_2$ to $CdCl_2$ in the solution.

In this phase, we have conducted a study of the effects of the zinc content of the thin sulfide film on the cell performance. We have discovered a pronounced effect on the V_{oc} and fill factor. Sulfide films of different zinc contents were deposited by CBD onto substrates from different CIGS runs. Cells were made from these substrates with similar ZnO films after they were CBD-coated. The following table shows that the gallium content in the CIGS layers are essentially the same for all samples. There is no detectable correlation between I/III ratio (within this limited range) and either V_{oc} or fill factor. Voltage performance does correlate strongly with the zinc content in the sulfide layer, with better results exhibited by cells with 20% zinc than for those with 30% zinc.

Table 3-1. Performance of $ZnO/Cd_{1-y}Zn_yS/CuIn_{1-x}Ga_xSe_2$ cells with varied gallium (x) and zinc (y) molar fractions

CIGS#	[I]/[III]	Ga content x (%)	Zn content y (%)	V_{oc} ^a (volt)	FF ^a
1508A	0.894	27	30	.4364	.5846
1508B			20	.4668	.6295
1516A	0.876	26	30	.5210	.6021
1516B			20	.5337	.6744
1517A	0.899	29	30	.4627	.6031
1517B			20	.5138	.6120
1518A	0.863	25	30	.4455	.6136
1518B			20	.4808	.6313
1519A	0.881	25	30	.4936	.6275
1519B			20	.5345	.6375

^amean value of four cells from the same substrate at quasi-steady state (light-soaked for 5 minutes)

From these results we can conclude that zinc content in the sulfide film is an important factor for the optimization of high efficiency CIGS cells. We cannot yet ascertain whether the results reported here are indicative of inherent properties of the $CdZnS/CuInGaSe_2$ interface or limitations of the CBD process when higher zinc content is incorporated into the CdZnS film.

3.1.3 ZnO Layer

The ZnO layer is a high resistivity/low resistivity bilayer. The reasons for using the bilayer and the method used for adjusting the resistivity of the two layers are unchanged from that described in previous reports [4, 5]. The ZnO is deposited by RF magnetron sputtering from a target doped with Al₂O₃ using argon or an oxygen/argon mix to control the resistivity and optical clarity. The total thickness of the ZnO layer for the present cells is approximately 0.37 micron, thinner than the 0.65 micron reported for previous cells. The sheet resistance is comparable to that previously obtained, 28 ohms/square, indicating lower bulk resistivity material.

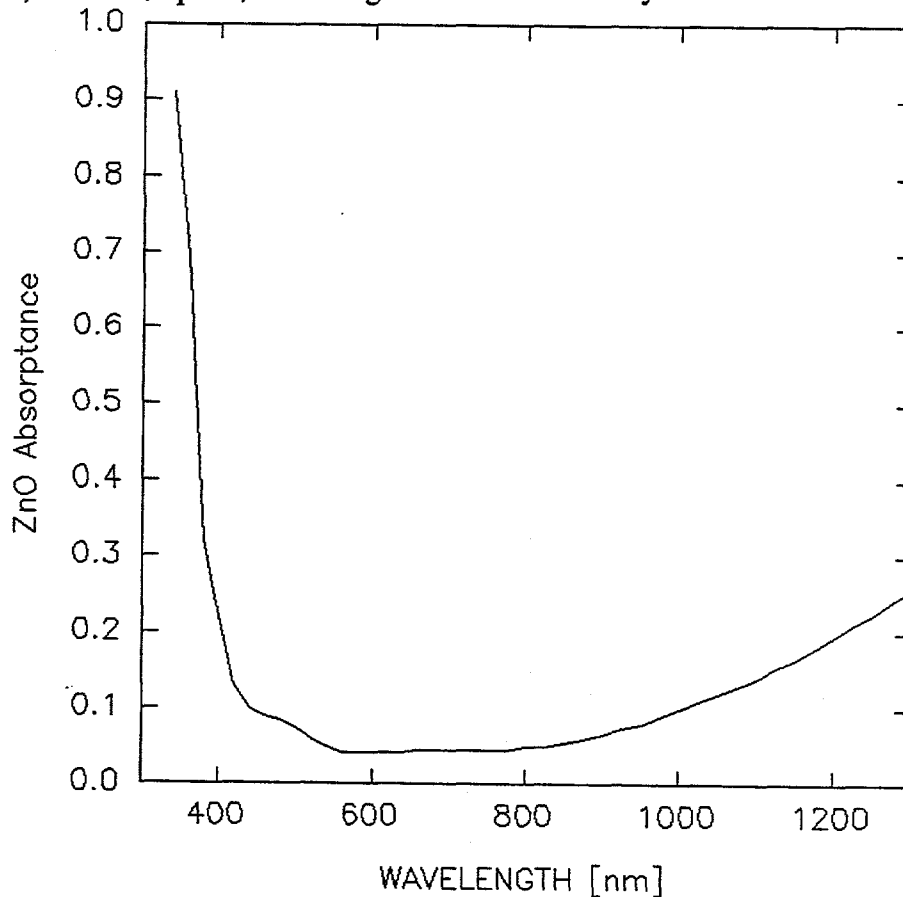


Figure 3-3. Optical absorption of the ZnO layer as used in the high efficiency cells. Derived from measurement of diffuse + specular reflectance and transmission on a P-E Lambda-9.

The optical absorption of the ZnO layer as used in the high efficiency cells has been inferred from transmission measurements on witness layers deposited on glass. We have previously confirmed that such witness layers do indeed give values applicable to the ZnO layers deposited on cells. Figure 3-3 shows the ZnO absorption for the 28 ohms/square film used on the best cells. Both infrared absorption due to free carriers and an overall wavelength independent absorption are present. These optical results indicate that the lower bulk resistivity was achieved without any loss of optical transmission. The effects of this absorption on cell performance are discussed below.

3.2 DEVICE ANALYSIS

3.2.1 Light Generated Current

The I-V characteristics and derived parameters as measured at NREL of the best cell fabricated during the present work (# 1490AD) were shown previously in figure 1-2. The test conditions were 100 mW/cm^2 equivalent intensity, AM1.5 global spectrum and 25°C sample temperature. The cell measures 13.1% under these test conditions with $V_{oc} = 0.518$ volts, $I_{sc} = 34.1$ mA, $FF = 0.728$ and a cell area of 0.979 cm^2 .

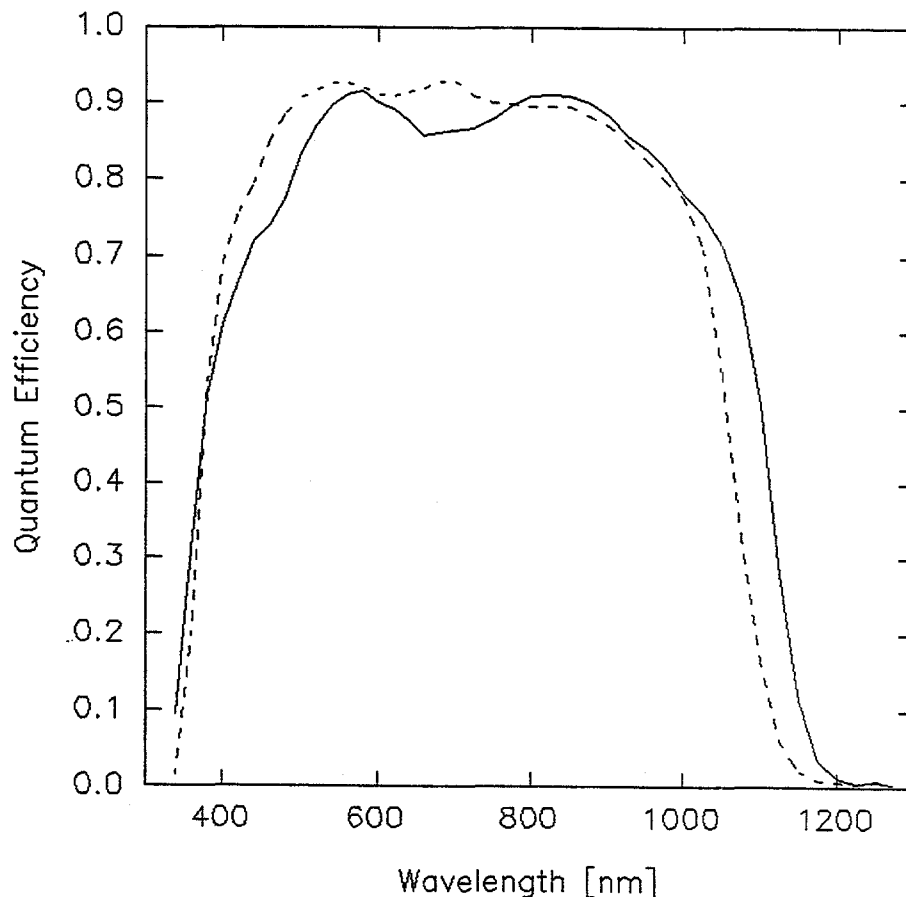


Figure 3-4. Quantum Efficiency of Cell 1490AD with 20% gallium (solid line) compared with cell 1174H with 28% gallium (dashed line).

Figure 3-4 shows the quantum efficiency of this same cell as measured at Boeing. The measurement is at short circuit electrical bias and was found to be independent of any applied light bias. In the figure the cell is compared to our previous best cell [5]. This comparison shows several features of the present cells. The shift of the long wavelength absorption edge is due to the lower gallium content of the present cell, approximately 20% as compared to 28% for the previous cell. The structure in the quantum efficiency between the selenide absorption edge and the window cutoff is primarily the coherent optical interference in the ZnO layer. The offset in the interference pattern between the two curves is due to the difference in thickness between the ZnO layers (cf: section 3.1.3).

We have quantified the optical losses in these cells by measuring the cell reflection and the ZnO absorption for a second cell fabricated on the same substrate as the high efficiency cell described above. Figure 3-5 shows the quantum efficiency and reflectance of this second cell along with several derived curves. Reflectance for this cell is the bottom-most curve shown in figure 3-5. The grid coverage accounts for approximately 0.02 of this reflectance and has little wavelength dependence. The structure seen in the curve is the effect of the optically coherent ZnO layer. The quantum efficiency of this cell is the second curve from the bottom, and is essentially identical to that of the high efficiency cell described above. There is a slight shift in the selenide absorption edge, probably due to gradients in the gallium content across the original substrate. There is also a slight wavelength shift in the interference peaks due to a small ZnO layer thickness difference but the conclusions obtained still apply equally well to both cells.

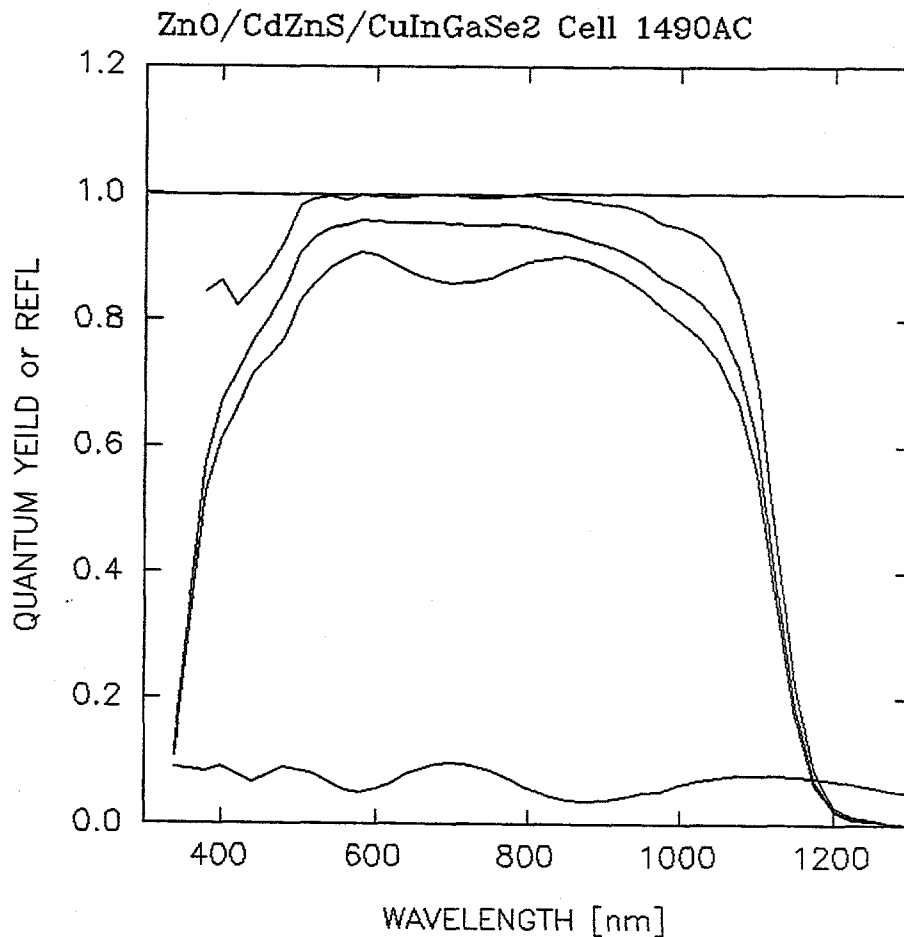


Figure 3-5. Cell 1490AC reflectance and quantum efficiency. The various curves are identified in the text.

The third curve from the bottom in figure 3-5 corrects the quantum efficiency for this reflection loss. Essentially all structure is removed, as expected.

Removal of the ZnO absorption results in the top curve in figure 3-5, which within the limits of accuracy of the measurement is equal to unity over much of the wavelength region. The remaining losses at short circuit are the CdZnS absorption at short wavelength and the CuInGaSe₂ collection losses at long wavelength.

The CdZnS layer is thin enough to give approximately 80% optical transmission above the sulfide band edge, we estimate it is 20 nm thick on the best cell reported here. Zinc content in the sulfide is as reported previously, approximately 0.18 expressed as the Zn/(Zn+Cd) mole fraction.

Table I shows a summary of the power losses in the cell expressed as the fractional increase available if the loss were reduced to zero. In order to allow comparison with the effect of changes in fill factor the increase is expressed as the percent increase in power output (and therefore efficiency) referenced to the AM1.5G measured power normalized to 100%.

Table 3-2. The effect on efficiency of removing the major quantified loss mechanisms in the present cells, as measured on cell #1490AC.

Loss mechanism	Relative power gain
Reflection	+5.0%
Grid shadowing losses	+2.2%
ZnO Optical Losses:	
Wavelength independent absorption:	+4.5%
ZnO bandedge	+1.7%
IR absorption (free carrier)	+1.8%
CdZnS absorption(no ZnO)	+1.8%
Selenide IR rolloff	+2.4%
ZnO sheet resistance loss ^a	+0.3%
Grid resistance losses ^a	+1.4%

^acalculated

3.2.2 Open Circuit Voltage

We observe a slight decrease in bandgap and in V_{oc} as expected in shifting from 28% gallium to 20% gallium. At first glance the V_{oc} loss appears favorable since it is considerably less than the band gap shift. The band gaps of the two cells are 0.045 eV shifted from comparison of the quantum efficiency curves. The Measured V_{oc} difference is 0.037 V. However, in general we have seen a gain in V_{oc} of approximately 2/3 of the band gap shift with the incorporation of gallium into the selenide. The V_{oc} of the 20% gallium content cell is in fact slightly lower than what would be predicted from this rule when compared with the 28% gallium cell. Therefore little change in the fundamental mechanisms controlling V_{oc} has been made in our improvement from 12.5% to 13.1% efficiency.

Table 3-3 shows the I-V parameters as measured at Boeing of the 4 cells made on the substrate which yielded the highest efficiency. Their I-V curves' slopes at short circuit indicate that the large difference in V_{oc} is not accompanied by corresponding shunt problems. Quantum efficiency measurements indicate little variation in ZnO or CdZnS layer characteristics across the substrate. These results taken together indicate that electronic variations resulting from fairly subtle compositional or structural differences (perhaps resulting from thermal gradients; cf: section 3.1.1), have a large effect on open circuit voltage.

Table 3-3. Current-Voltage characteristics of the 4 cells made on the substrate which yielded the highest efficiency

Cell	V _{oc} [V]	I _{sc} [mA]	FF	Efficiency ^a (%)
1490AA	0.455	33.5	0.681	10.5
1490AB	0.433	34.2	0.658	9.8
1490AC	0.429	33.5	0.669	9.6
1490AD	0.513	34.1	0.728	12.7

^aTests conducted at Boeing at 25°C, approximately 100 mW/cm², AM1.5G spectrum. For calibrated test of cell 1490AD see figure 1-2. All areas are assumed 1 cm².

3.2.3 Fill Factor

The fill factor of the best cell we have fabricated in this first phase of this contract (0.728) is considerably higher than that of our previous best device (0.657). The major cause is absence of the local shunting paths present in most of the earlier thin sulfide cells. This shunting is believed to have been due to contact between the ZnO layer and the selenide layer at multiple defects in the thin sulfide layer. A simple estimating procedure suggested that on the order of 1% of the net cell area consisted of ZnO/CuInGaSe₂ contact. While the preparation method for the sulfide film has not been substantially changed, improvements in the application technique have resulted in more reproducible deposition conditions and in smoother, more continuous films. This has resulted in the reduced shunting observed in these devices.

The shunt improvement alone is not sufficient to explain all of the increase in fill factor. In terms of a lumped parameter equivalent circuit model the series resistance is much lower for this cell. This is at present believed to be a bulk selenide effect.

After removal of these mechanisms there are still several identifiable loss mechanisms present in the fill factor. These are ZnO sheet resistance losses, and grid resistance losses, whose calculated values are included in table 3-2.

4.0 CONCLUSIONS

Table 3-2 quantifies several clear paths to further efficiency improvement. There is no longer a single dominant loss mechanism to attack since the light generated current losses (collectively the largest category) are well understood. In addition, the fill factor is improving as we identify the mechanisms controlling it. However, significant improvement is still possible via several means:

- 1) The simplest method for reducing the reflection losses in the cell and thereby validating the estimate of losses made above is to apply a quarter wave coating of MgF_2 . This prediction has been tested and shown to provide 2-3% improvement in current. Further reduction would probably be difficult because of the coherent optical interference in the ZnO layer. A similar improvement could be realized using a coverglass and refractive index matching layers, but would be more complicated and unnecessary for the demonstration of higher efficiency intended here.
- 2) Because ZnO sheet resistance voltage losses in this cell are so low, simply using thinner layers of our current ZnO material to reduce parasitic absorption loss of photocurrent will result in lower net loss. Furthermore, significant efficiency increases can come from improvements in the electro-optical characteristics of the ZnO. Higher carrier mobility and decreased carrier density, perhaps resulting from improved electrical activation of dopants, should allow significant reductions in the ZnO absorption, especially the wavelength independent losses.
- 3) Clear improvement in the IR rolloff of the selenide current collection was achieved in the present phase of this contract and further improvement in minority carrier collection should reduce this loss further.

Increased gallium content in the selenide should result in improved efficiency if the other material parameters are not significantly degraded and the observed trend in voltage increase with bandgap persists to even higher levels.

Most importantly, in absolute terms open circuit voltage as a fraction of the selenide bandgap is still low. The fundamental limits on V_{oc} are tied to forward current recombination mechanisms, which in high efficiency cells are most probably dominated by bulk recombination in the space charge region. We are still unable to identify the controlling recombination centers, or even to specify whether they are located within the individual grains of the polycrystalline absorber or on the grain boundaries. Hence, though not quantifiable in the same manner as the understood mechanisms identified in table 3-2, the greatest improvements in efficiency are still to come from circumventing the mechanisms limiting the voltage.

Our plans for Phase 2 include: a methodical study of thermal and composition gradients in our CIGS evaporator to elucidate the factors controlling the performance variations observed across individual substrates; an effort to identify the uncontrolled factors affecting the reproducibility of the CdZnS CBD process; and development of an economical reactive sputtering process for device-quality ZnO utilizing a new rotating-cathode source.

5.0 REFERENCES

1. W.S. Chen, J.M. Stewart, B.J. Stanbery, W.E. Devaney, and R.A. Mickelsen, "Development of Thin Film Polycrystalline $\text{CuIn}_{(1-x)}\text{Ga}_x\text{Se}_2$ Solar Cells," The Conference Record of the 19th IEEE Photovoltaic Specialists Conference, 1987, pp. 1445-1447.
2. W.E. Devaney, W.S. Chen and J.M. Stewart, "High Efficiency CuInSe_2 and CuInGaSe_2 Based Cells and Materials Research," Final Technical Progress Report, Contract ZL-8-06031-8, May, 1990.
3. H.A. Macleod, Thin-Film Optical Filters, New York: American Elsevier Publishing Company, Inc., 1969.
4. W.E. Devaney, W.S. Chen and J.M. Stewart, "High Efficiency CuInSe_2 and CuInGaSe_2 Based Cells and Materials Research," First Annual Technical Progress Report, Contract ZL-8-06031-8, April, 1989.
5. W.E. Devaney, W.S. Chen, J.M. Stewart and R.A. Mickelsen, "Structure and Properties of High Efficiency $\text{ZnO}/\text{CdZnS}/\text{CuInGaSe}_2$ Solar Cells," IEEE Transactions Electron Devices, Vol. 37, No. 2, pp. 428-433.

ABSTRACT

Analysis of the properties of the best ZnO/CdZnS/CuInGaSe₂ cells developed by Boeing for SERI under a prior subcontract suggested that significant performance improvements could be realized by further optimization of the thin CdZnS layer to reduce shunt currents while maintaining subbandgap transparency, the ZnO layer to reduce IR absorption while maintaining adequate lateral conductivity, and the CuInGaSe₂ (CIGS) layer to optimize gallium content and gradients along with minority carrier transport properties.

During this contract phase our CIGS deposition system was modified to double its substrate capacity. Second, new tooling was developed to enable investigation of a modified aqueous CdZnS process whose goal was to improve the yield of this critical step in the device fabrication process. Third, our ZnO sputtering system was upgraded to improve its reliability, and the sputtering parameters further optimized to improve its properties as a Transparent Conducting Oxide (TCO).

Combining the refined CdZnS process with CIGS from the newly fixtured deposition system enabled us to fabricate and deliver an 11.5% efficient, 4 cm², CuIn_{0.71}Ga_{0.29}Se₂ cell. Further refinement of both the CIGS and TCO deposition processes has enabled us fabricate a ZnO/Cd_{0.82}Zn_{0.18}S/CuIn_{0.80}Ga_{0.20}Se₂ cell whose I-V characteristics and derived parameters as measured at NREL under standard test conditions gave 13.1% efficiency with V_{oc} = 0.518 volts, I_{sc} = 34.1 mA, FF = 0.728 and a cell area of 0.979 cm². This NREL measurement verifies that we have met our key technical milestone for Phase 1. Furthermore, we have delivered to NREL 6 each ~1 cm² CuIn_{1-x}Ga_xSe₂ cells which are 12-13% in efficiency with gallium contents in the range 0.20 ≤ x ≤ 0.26.

Analysis of the electrical and optical properties of devices fabricated during this phase has led to the identification of several clear paths to further efficiency improvement which will be pursued in the course of Phase 2 of this contract.

Document Control Page	1. NREL Report No. NREL/TP-413-5012	2. NTIS Accession No. DE92016439	3. Recipient's Accession No.
4. Title and Subtitle Research on Polycrystalline Thin-Film CuGaInSe ₂ Solar Cells		5. Publication Date November 1992	
		6.	
7. Author(s) B.J. Stanbery, W.S. Chen, W.E. Devaney, J.W. Stewart		8. Performing Organization Rept. No.	
9. Performing Organization Name and Address Boeing Defense & Space Group P.O. Box 3999, M.S. 9E-XX Seattle, Washington 98124-2499		10. Project/Task/Work Unit No. PV231101	
		11. Contract (C) or Grant (G) No. (C) ZH-1-19019-6 (G)	
12. Sponsoring Organization Name and Address National Renewable Energy Laboratory 1617 Cole Blvd. Golden, CO 80401-3393		13. Type of Report & Period Covered Technical Report 3 May 1991 - 2 May 1992	
		14.	
15. Supplementary Notes NREL technical monitor: H.S. Ullal			
16. Abstract (Limit: 200 words) This report describes research to fabricate high-efficiency CdZnS/CuInGaSe ₂ (CIGS) thin-film solar cells, and to develop improved transparent conductor window layers such as ZnO. A specific technical milestone was the demonstration of an air mass (AM) 1.5 global, 13% efficient, 1-cm ² -total-area CIGS thin-film solar cell. Our activities focused on three areas. First, a CIGS deposition system was modified to double its substrate capacity, thus increasing throughput, which is critical to speeding the process development by providing multiple substrates from the same CIGS run. Second, new tooling was developed to enable an investigation of a modified aqueous CdZnS process. The goal was to improve the yield of this critical step in the device fabrication process. Third, our ZnO sputtering system was upgraded to improve its reliability, and the sputtering parameters were further optimized to improve its properties as a transparent conducting oxide. The characterization of the new CIGS deposition system substrate fixturing was completed, and we produced good thermal uniformity and adequately high temperatures for device-quality CIGS deposition. Both the CIGS and ZnO deposition processes were refined to yield a ZnO/Cd _{0.82} Zn _{0.18} S/CuIn _{0.80} Ga _{0.20} Se ₂ cell that was verified at NREL under standard testing conditions at 13.1% efficiency with V _{oc} = 0.581 V, J _{sc} = 34.8 mA/cm ² , FF = 0.728, and a cell area of 0.979 cm ² .			
17. Document Analysis a. Descriptors polycrystalline ; thin films ; photovoltaics ; solar cells ; copper ; gallium ; Indium ; selenide b. Identifiers/Open-Ended Terms c. UC Categories 273			
18. Availability Statement National Technical Information Service U.S. Department of Commerce 5285 Port Royal Road Springfield, VA 22161		19. No. of Pages 23	
		20. Price A03	